NUMERICAL INVESTIGATION OF TRANSITION CONTROL IN LOW CONDUCTIVE FLUIDS

T. Albrecht[1], *R. Grundmann*[1], *G. Mutschke*[2], *G. Gerbeth*[2]

[1] *Institute for Aerospace Engineering, Dresden University of Technology, D-01062 Dresden (albrecht@tfd.mw.tu-dresden.de)*
[2] *MHD Department, Institute of Safety Research, Forschungszentrum Rossendorf, P.O. Box 51 01 19, D-01314 Dresden*

Introduction. We investigate by two- and three-dimensional direct numerical simulation (DNS) and linear stability analysis (LSA) the transition to turbulence in a flat-plate boundary layer controlled by a steady, wall-parallel and streamwise orientated Lorentz force. The fluid considered is incompressible, Newtonian and low-conductive. Using a free-stream velocity U_∞ and an inflow displacement thickness δ_1 to nondimensionalize the Navier–Stokes equations, the Lorentz force term reads $f_l = (\mathrm{Z}\,a^2)/(\pi^2\mathrm{Re})exp(-\pi y/a)$, where a is the actuator's nondimensional spacing of electrodes and magnets, Re is the Reynolds number (based on δ_1), and Z is a modified Hartmann number [1], describing the ratio of Lorentz and viscous forces. If $\mathrm{Z} = 1$, any initial Blasius velocity profile will evolve towards an exponential one, thereby gaining a critical Reynolds number, which is increased by two orders of magnitude, as suggested first by Gailitis and Lielausis [2] in the early 1960s. In this paper, we address the question about the stability properties of the intermediate profiles. Hereby, we restrict to the case of shortest transition length from Blasius to an exponential profile, which occurs at $\delta_1^{\mathrm{Blasius}}/\delta_1^{\mathrm{exp}} \approx 1.4$ [3].

1. Two-dimensional DNS.

1.1. Numerical method. To investigate the impact of the Lorentz force on Tollmien–Schlichting (TS) waves, we first performed 2D simulations based on a spectral element method by Karniadakis [4]. The rectangular computational domain extending over 990 δ_1 in streamwise direction and 65 δ_1 in wall-normal direction was decomposed into 594 elements of polynomial degree 9. Reynolds number is chosen to 360, and the electromagnetic actuator at the bottom wall starts 200 units from inflow at $\xi = 0$ towards the outflow boundary where $\xi = \pi^2(x - 200)/(a^2\mathrm{Re})$ denotes a new shifted streamwise coordinate used in the following. Boundary conditions include a Blasius velocity profile at inflow, no-slip condition $\mathbf{u} = 0$ at bottom wall, and outflow condition $(\mathbf{n} \cdot \boldsymbol{\nabla})\mathbf{u} = 0$ at both downstream and free-stream boundary. Small amplitude disturbances $0.4 \leq \mathrm{F}^+ \leq 3.5$ of nondimensional frequency $F^+ = (2\pi f\nu/U_\infty^2) \times 10^4$ are introduced near the inflow from which TS waves evolve. A sponge region technique [5] prevents unphysical reflections of small scale velocity fluctuations at the outflow boundary.

1.2. Results. In uncontrolled case TS waves grow and decay corresponding to non-parallel linear stability theory. Already when applying a compareably small Lorentz force $\mathrm{Z} = 0.05$, TS waves of all investigated frequencies are damped within the computational domain. For the case $\mathrm{Z} = 1$ shown in Fig. 1, the growth rate, based on the maximum root mean square value over wall-normal direction of the streamwise velocity component, is minimum in a region near the onset of control and increases as the velocity profile approaches the exponential state.

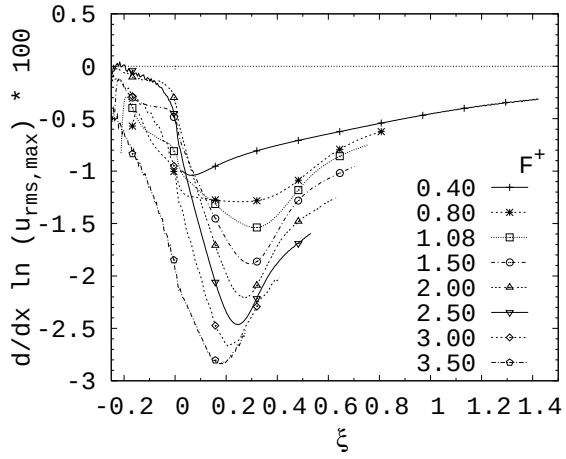

Fig. 1. Evolution of TS wave growth rates for selected frequencies during transition from Blasius to exponential profile.

2. Linear Stability Analysis. In order to get further insight into the (temporal) stability behavior of the intermediate (local) velocity profiles, a linear stability analysis has been performed. Assuming small velocity disturbances $\Phi(y)\mathrm{e}^{i\alpha(x-ct)}$ to a base profile $U(y)$, linearization leads to the Orr–Sommerfeld equation. Hereby, real values of α and the real part of c denote wave number and phase velocity of the disturbance, respectively. Negative imaginary parts of c then signal instability of the profile. The boundary conditions are that the disturbance and its first derivative have to vanish at $y = 0$ and $y \to \infty$.

2.1. Numerical method and validation. We have implemented a Chebyshev tau method based on the modifications described by Gardner *et al.* [6] to avoid spurious eigenvalues. An exponential mapping $x = 2\,\mathrm{e}^{-\rho y} - 1$ transforms between the semi-infinite wall-normal coordinate y and the Chebyshev interval $[-1, 1]$ of the new coordinate x. Hereby, ρ denotes an additional mapping parameter. The discretization procedure results in a generalized eigenvalue problem of expansion order $N-2$ which has been solved by a standard LAPACK procedure. Extensive resolution tests and validation runs for both the Blasius boundary layer profile and the exponential velocity profile have been performed ensuring the accuracy of the method. The critical Reynolds number of the exponential profile $U(y) = 1 - \mathrm{e}^{-y}$

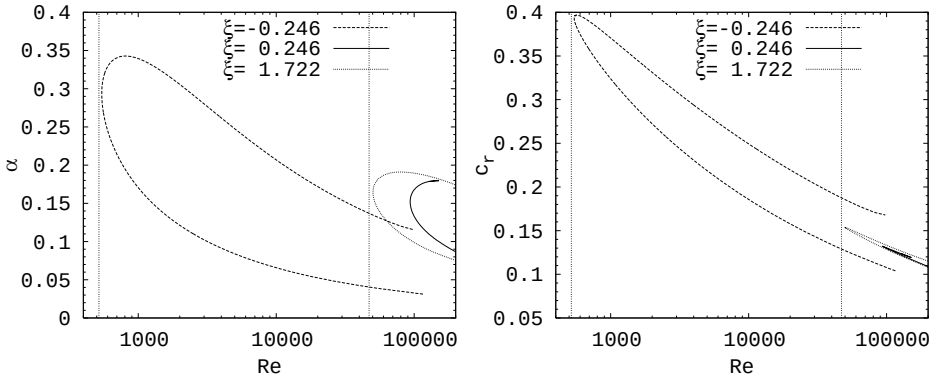

Fig. 2. Curves of neutral stability vs. the Reynolds number at three downstream locations: $\xi = -0.246$ (close to the Blasius profile), $\xi = 0.246$ (during transition) and $\xi = 1.722$ (almost exponential). Left: wave number α, right: phase velocity c_r.

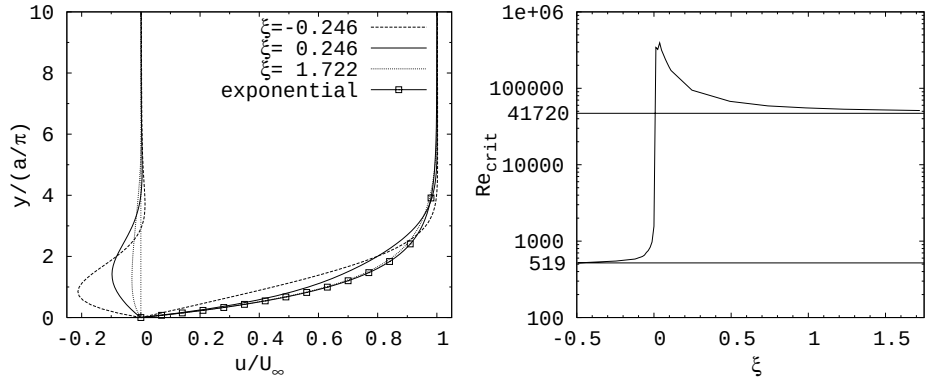

Fig. 3. Left: velocity profiles at three downstram locations (see Fig. 2). At $u/U_\infty = 0$, additionally the deviation from the exponential profile is shown. Right: critical Reynolds number vs. the downstream coordinate. The Lorentz force starts beginning from $\xi = 0$.

has been found to $\mathrm{Re}_\mathrm{c}^\mathrm{exp} = 47119.5$ at $\alpha_c = 0.16225$ and $c_r = 0.15586757$ at $N = 102$ and $\rho = 0.1$ which is in good agreement to results of Priede [7] and Lakin & Reid [8].

2.2. Results. The analysis has been applied to velocity profiles originating from the above DNS. As the Lorentz force is switched on at $\xi = 0$, Fig. 2 shows curves of neutral stability vs. Reynolds number at three different downstream locations. Upstream the Lorentz actuation at $\xi = -0.246$, the profile is close to the Blasius shape (because of a small upstream influence due to the elliptic nature of the Navier–Stokes equations), resulting in a critical Reynolds number only slightly above $\mathrm{Re}_\mathrm{c}^\mathrm{Blasius} = 519$ (vertical dotted line). Far downstream, at $\xi = 1.722$, the profile is almost exponential, resulting in a critical Reynolds number slightly above $\mathrm{Re}_\mathrm{c}^\mathrm{exp}$ (vertical dotted line). However, downstream the onset of the force at $\xi = 0.246$, the critical Reynolds number is clearly larger than $\mathrm{Re}_\mathrm{c}^\mathrm{exp}$.

Fig. 3 shows the corresponding velocity profiles (additionally, their deviations from the exponential profile) and the behavior of the critical Reynolds number vs. the downstream coordinate ξ. The action of the Lorentz force leads to intermediate velocity profiles, which are more stable than the asymptotically reached exponential profile.

Recent LSA results of a velocity profiles extracted from the simulation of the boundary layer equations obtained by a Chebyshev collocation method show similar results [9].

3. Three-dimensional DNS. For 3D DNS, the domain size is 26 δ_1 in the homogeneous, periodical spanwise direction, allowing for a Fourier ansatz for pressure and velocity where up to 128 modes were used. Fig. 4 shows vortex visualization by means of the λ_2 method [10] of the predicted flow when applying different Lorentz force amplitudes $0 \leq \mathrm{Z} \leq 1$. The growth of 3D disturbances due to the secondary instability mechanism is clearly visible since Λ-vorticies form in all cases, even though their intensity (vorticity) lowers as Z is increased. In uncontrolled case Ω-vorticies emerge, followed by a rapid breakdown to turbulence. This process is delayed when applying a moderate Lorentz force ($\mathrm{Z} = 0.1$) or even stopped for $\mathrm{Z} \geq 0.2$, where Λ-vorticies remain stable and dissipate downstream.

4. Discussion. DNS and LSA results confirm the expected increased stability of the controlled flow. Depending on Lorentz force strength transition to turbulence is delayed or even stopped. Surprisingly, both DNS and LSA results suggest interesting stability characteristics of the intermediate velocity profiles

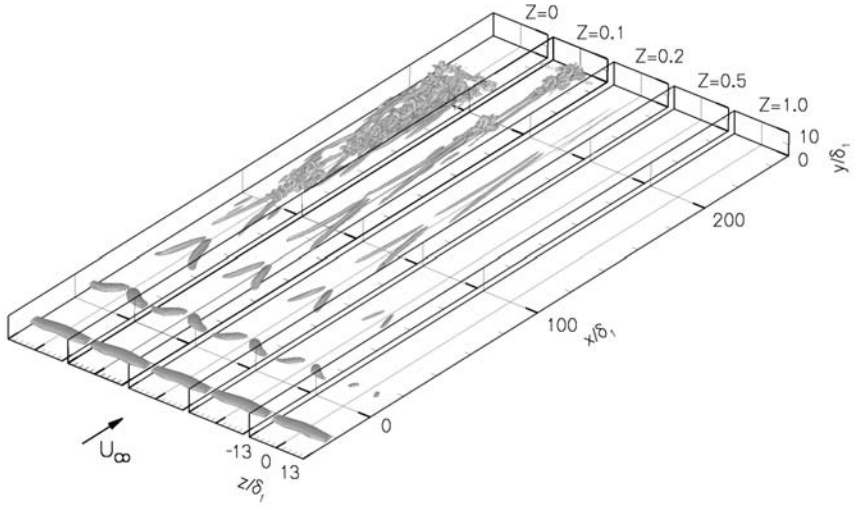

Fig. 4. Transition to turbulence controlled by the Lorentz force.

investigated here. We would like to mention that critical Reynolds numbers larger than the one for the exponential profile were also found in other problems [11], and supercriticality of the exponential suction profile as found by Hocking [12] gives some support to our results.

By three-dimensional DNS we show that transition to turbulence can be stopped even in its late stage. While the evolution of Λ-vortices from former two-dimensional TS waves remains almost unchanged, the emerge of Ω-vortices is supressed with increasing Lorentz force strength, thus relaminarizing the flow.

5. Acknowledgement. We are grateful to Janis Priede and Tom Weier for many fruitful discussions and thank Prof. G. Karniadakis for the donation of the spectral element code.

REFERENCES

1. T. Weier, U. Fey, G. Gerbeth, G. Mutschke, V. Avilov. *ERCOFTAC Bulletin*, vol. 44 (2000), pp. 36–40.
2. A. Gailitis, O. Lielausis. *Applied Magnetohydrodynamics, Reports of the Physics Institute Riga*, vol. 12 (1961) pp. 143–146 (in Russian).
3. E. Kneisel, Boundary layer control by electromagnetic forces., Kleiner Beleg, TU Dresden/FZ Rossendorf, 2004 (in German).
4. R.D. Henderson, G.E. Karniadakis. *J. Comp. Phys.*, vol. 122 (1995), pp. 191–217.
5. Y. Guo, N. A. Adams, L. Kleiser. *AIAA J.*, vol. 34 (1996), pp. 683–690.
6. D.A. Gardner, S.A. Trogdon, R.W. Douglass. *J. Comp. Phys.*, vol. 80 (1989) pp. 137–167.
7. J. Priede, private communication, 2005.
8. W.D. Lakin, W.H. Reid. *J. Mech. appl. Math.*, vol. XXXV, Pt.1 (1982) pp. 69–89.
9. E. Kneisel, Linear stability analysis of velocity profiles of flat plate boundary layer flow controlled by Lorentz forces. Internal Report, FZ Rossendorf, 2004 (in German).
10. J. Jeong, F. Hussain. *J. Fluid. Mech.*, vol. 285 (1995), pp. 69–95.
11. M.I. Zhilyaev, T. A. Khmel' and V. I. Yakovlev. *Magnitnaya Gidrodinamika* vol. 27 no. 2 (1991) 76-83 (in Russian).
12. L.M. Hocking, *Quart. J. Mech. Appl. Maths* vol. 28 (1975) pp. 341–353.